Supporting Information

Tailoring drug release profile of hydrogels formed from low-molecular-weight compounds by supramolecular co-assembly and controlled thiol-ene orthogonal coupling

David Díaz Díaz,*[a,b] Emmanuelle Morin,[c,d] Eva M. Schön,[a] Ghyslain Budin,[d] Alain Wagner[d] and Jean-Serge Remy[c]

[a] *Institut für Organische Chemie, Universität Regensburg, Universitätsstr. 31, 93040 Regensburg, Germany*

[b] *Instituto de Ciencias de Materiales de Aragón, CSIC-Universidad de Zaragoza, Pedro Cerbuna 12, 50009 Zaragoza, Spain*

[c] *Chimie Génétique, Faculté de Pharmacie, 67000 Strasbourg, France*

[d] *Laboratory of Functionnal ChemoSystems, UMR 7199, Faculté de Pharmacie, 67000 Strasbourg, France*

David.Diaz@chemie.uni-regensburg.de

Contents List

1. Synthesis of compounds

- ***General remarks***

^{1}H and ^{13}C NMR spectra were obtained at 25 ºC on a BRUKER AC-300 instrument. Chemical shifts are denoted in δ units (in ppm) relative to tetramethylsilane (TMS) as internal standard or relative to residual solvent peaks. IR spectra were recorded using a Diamond ATR (attenuated total reflection) accessory (Golden Gate) on a Bio-Rad Excalibur FTS 3000 MX spectrophotometer. MS (ESI) spectra were obtained from an Agilent 6460 Triple Quadrupole LC/MS instrument. Melting points (mp) were measured in a Büchi 504392-S or Opti Melt MPA 100 equipment and are uncorrected. Elemental analyses were performed with a Perkin-Elmer 2400 CHN equipment. Fourier Transform Infrared (FT-IR) spectra of solid samples were obtained at room temperature using a FTS 3000 MX spectrophotometer equipped with a high-pressure diamond ATR accessory. *L*-Cystine (CAS Number: 56−89−3) and *N*,*N*′-Dibenzoyl-*L*-cystine (**1**) (CAS Number: 25129−20−8) were purchased from Sigma-Aldrich Co. *N*,*N*′-Diacryloyl-*L*-cystine (**3**) was obtained in 25% yield as a white solid starting from *L*-cystine (0.5 g, 2.1 mmol) and following the procedure described in the literature, displaying spectroscopic data consistent with those reported.[1] Vinyl-containing analogues **2** and **4** were synthesized via standard Schotten-Baumann *N*-acylation of *L*-cystine.[2,3] 4-Methoxy-hydroquinone was used as radical inhibitor during the synthesis of compounds. Unless otherwise indicated, necessary solvents and reagents were purchased of p.a. grade and used as received without further purification.

- ***Synthesis and characterization***

N,*N*′-Di[4-(3-butenyl)benzoyl)]-*L*-cystine (**2**): 4-3-(butenyl)benzoic acid (1.0 g, 5.7 mmol) was dissolved in freshly distilled thionyl chloride (0.7 mL, 9.6 mmol) and stirred for 2 h and further refluxed for 30 min. Removal of the excess thionyl chloride under reduced pressure afforded the corresponding 4-3-(butenyl)benzoyl chloride, which was used for the next reaction without further purification. A three-necked, 100 mL round-bottom flask was charged with *L*-cystine (0.48 g, 2.0 mmol), methoxy hydroquinone (5 mg), Et_2O (2 mL) and water/EtOH (6 mL, 95/5 v/v) and equipped with a stirrer, a thermometer, and two 25 mL pressure-compensated addition funnels. One funnel was charged with 2 N NaOH (4.6 mL) and the other one with 4-3-(butenyl)benzoyl chloride (0.86 g, 4.4 mmol) dissolved in Et_2O (0.5 mL). The mixture was cooled to 0 ºC in an ice bath and the two funnels discharged dropwise under vigorous stirring over 3 h in order to keep the temperature always below 5 ºC. After the addition, the reaction mixture was allowed to warm slowly to room temperature and stirred for additional 5 h. Then, the reaction mixture was acidified until pH 1−2 with 10 N HCl aqueous solution. Water was removed by three freeze-drying cycles under reduced pressure and the obtained white solid was suspended in dry acetone and vigorously stirred for 30 min. The resulting suspension was filtered and the filtrate evaporated under reduced pressure to afford **2** as a white solid, which was further purified by trituration/filtration in Et_2O (228 mg, 21% yield): ^{1}H NMR (300 MHz, DMSO-d_6) δ/ppm = 2.22−2.35 (m, 4H), 2.68−2.76 (m, 4H), 3.10−3.26 (m, 2H), 3.24−3.34 (m, 2H), 4.64−4.72 (m, 2H), 3.75 (br s, 2H), 4.93−5.04 (m, 4H), 5.73−5.87 (m, 2H), 7.27 (d, J = 8 Hz, 4H), 7.78 (d, J = 8 Hz, 4H), 8.77−8.80 (br s, 2H); ^{13}C NMR (75 MHz, DMSO-d_6) δ/ppm = 34.1, 34.5, 39.1, 51.7, 115.3, 127.3, 128.1, 131.2, 137.6, 145.1, 166.2, 172.1; FT-IR ν_{max} (cm^{-1}) 3058−3313 (N−H stretching; overlap O−H stretching, acid band), 2931, 1742, 1653 (C=O stretching, amide I band), 1536 (N−H bending, amide II band), 1435, 1368, 982, 697; MS (ESI) *m/z* 557 [MH^+]. Elemental analysis calculated for $C_{28}H_{32}N_2O_6S_2$: C, 60.41; H, 5.79; N, 5.03; S. 11.52; found: C, 60.73; H, 5.86; N, 5.22; S. 11.19.

N,*N*′-Di(4-pentenoyl)-*L*-cystine (**4**): The same procedure used to obtain **2** was employed for the synthesis of **4** using *L*-cystine (0.5 g, 2.1 mmol) and 4-pentenoyl chloride (0.6 g, 5.1 mmol). Product **4** was isolated (161 mg, 19% yield) as a white solid: ^{1}H NMR (300 MHz, DMSO-d_6) δ/ppm = 2.21−2.24 (m, 8H), 2.91−2.99 (m, 2H), 3.11−4.07 (m, 2H), 4.48−4.57 (m, 2H), 4.92−5.05 (m, 4H), 5.76−5.85 (m, 2H), 8.35−8.42 (br s, 2H), 8.73 (br s, 2H); FT-IR ν_{max} (cm^{-1}) 3058−3320 (N−H stretching; overlap O−H

stretching, acid band), 2934, 1744, 1657 (C=O stretching, amide I band), 1537 (N–H bending, amide II band), 1435, 1371, 863, 687; MS (ESI) *m/z* 405 [MH^+]. Elemental analysis calculated for $C_{16}H_{24}N_2O_6S_2 \cdot$ ½ H_2O: C, 46.47; H, 6.09; N, 6.77; S. 15.51; found: C, 46.78; H, 6.23; N, 6.61; S. 15.32.

2. Gelation experiments and T_{gel} determination

- ***General remarks***

The gelation ability of *N*,*N*′-dibenzoyl-*L*-cystine (**1**) has been observed and studied by different groups.[2,4] The compound is known to be insoluble in pure water tending to crystallize, but it is readily soluble in most of the organic solvents. It represents one of the clearest examples of the delicate balance that exist between gelation and crystallization. The CH_2–S–S–CH_2 dihedral angle of about 90º plays a key role in the generation of the supramolecular network. DNA-like self-assembled structure is stabilized by cooperative hydrogen bonds between amide-NH and carboxyl-CO groups, as well as π-π staking interactions between parallel aromatic rings.[2] The practical minimum gelation concentration (MGC) of **1** in water was estimated as 0.2 wt.%. Lower concentrations of **1** lead too weak hydrogels, at least in our hands, to be accurately used during our experiments. The pH value for a 0.2 wt.% hydrogel made of **1** was ca. 3–4 (universal paper indicator). Surprisingly, our 0.2 wt.% hydrogels made of **1** (with and without entrapped 2-hydroxyquinoline, 1 mM) have always showed a much lower T_{gel} (ca. 2-fold lower) than the one reported somewhere else.[5] Nevertheless, we have not a clear explanation for this inconsistence yet.

In order to retain enough compatibility (hydrophobic/hydrophilic balance) during SMCA the non-covalent hydrogen-bonding pattern in **1** was maintained in analogues **2**–**4**, but the hydrophobic part of the amide groups was modified with terminal alkyne-containing units, which could still participate with π-π interactions during the molecular assembly and facilitate the further TEC cross-linking of the nanofibers. Nonetheless, such modifications shifted the tendency of the products towards dissolution or crystallization instead gelation over time.

Milli-Q-purified water (resistivity 18.2 mΩ) was used for the preparation of all hydrogels. The different mixtures displayed in Table 1 of the main paper at the indicated molar ratios were dissolved in water containing 0.5 wt.% DMSO as co-solvent upon heating. The formation of the corresponding hydrogels was observed upon cooling the isotropic solutions. Most of the so-formed gels were easily disrupted upon hand shaking. As expected, gel opacity increased with the concentration of [gelator + additives] system. In a typical gel preparation a weighted amount of the corresponding components were placed in a screw-capped pyrex glass vial (5 cm length and 1 cm diameter) together with 99.5% water/0.5% DMSO (1 mL). The mixture was gently heated with a heat-gun until the solids were completely dissolved. In order to keep constant the rate of further cooling, the temperature of the heat-gun was fixed to 120 ºC. The resulting solution was cooled down slowly to room temperature and left for 2 h, after which time the state of the solution was monitored visually by turning the test vial upside-down (Figure S1). The material was classified as "gel" if it did not exhibit gravitational flow. Before irradiation with UV-light (λ = 365 nm), the all samples were homogenised by placing them in a ultrasonic bath at 30 ºC for 2 min. After 10 min of irradiation the modified materials were purified and characterized. Purification of the hydrogels before their characterization and release studies was carried out as following: 1) the water from 1 mL samples was removed by freeze-drying; 2) the residue was triturated in a cold mixture water/Et_2O (1/1 v/v), filtered, and subsequently washed (x 2) with cold CH_3CN and Et_2O; 3) the resulting solid material was dried under reduced pressure for 24 h; and 4) the hydrogels were reformed by adding 1 mL of Milli-Q-purified water, heating to dissolve the solids and slow cooling at room temperature.

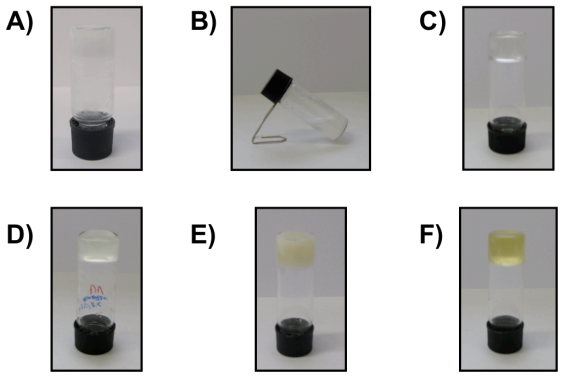

Fig. S1 Digital photographs of modified hydrogels as outlined in Table 1 of the main paper. Concentration **1** = 0.2 wt.% in 1 mL of 95.5% water:0.05% DMSO; molar ratio **1**:(**2**–**4**) = 10:1; molar ratio (**2**–**4**):(**5**–**6**) alkene groups:thiol groups = 1:1; 0.05 wt.% LAP. A) Gel made of [**1**+**2**] via SMCA; B) destruction by hand-shaking of gel made of [**1**+**2**+**6**] before TEC); C) reference gel made of **1**; D) gel made of [**1**+**2**+**5**] after SMCA-TEC; E) gel made of [**1**+**2**+**6**] after SMCA-TEC; F) gel made of [**1**+**4**+**6**] after SMCA-TEC.

- ***T_{gel} determination***

Gel-to-sol phase transition temperatures (T_{gel}) were determined by the inverse flow method. The temperature of the thermostated batch was raised at a rate of 2 ºC min^{-1}. T_{gel} was defined herein as the temperature at which the gel was broken. The experimental error of T_{gel} in at least two independent measurements was ± 3 ºC. All gels showed thermo reversibility, thus raising the temperature above the T_{gel} induced the gel-sol phase transition, and the solutions turned back to the gel states upon cooling at room temperature. Nevertheless, no clear thermal transitions were possible to observe by differential scanning calorimetry of the studied systems.

3. Cross-linking and control experiments

- ***General remarks***

Divalent, trivalent and tetravalent thiol-containing cross-linkers were purchased from Sigma-Aldrich Co.: 2,2′-(ethylenedioxy)diethanethiol (**5**, CAS number: 14970–87–7); trimethylolpropane tris(3-mercaptopropionate) (**6**, CAS number: 33007–83–9) and pentaerythritol tetrakis(3-mercaptopropionate) (**7**, CAS number: 7575–23–7) respectively. The water-soluble photoinitiator lithium phenyl-2,4,6-trimethylbenzoylphosphinate (LAP) was synthesized according to a described procedure and displayed identical spectroscopic data to those reported.[6]

Figure S2 shows the physical and chemical processes involved in the SMCA-TEC approach. The photochemically/thermally-induced version of the thiol-ene coupling reaction is known to proceed by a radical mechanism to give an anti-Markovnikov-type thioether. This process is rather inhibited by the presence of oxygen during the reaction as it happens for example with other free-radical reactions. In the former case the formed peroxy radical is still able to abstract a hydrogen from a new thiol and produce a new thiyl radical, which is added to the corresponding unsaturation. Several studies have demonstrated that the rate-determining step in the overall reaction is the abstraction of the thiol hydrogel by the carbon-centered radical rather than the addition of the thiyl radical to the olefine.[7] Among different photoinitiators used in similar TEC reactions in aqueous media (i.e. LAP, 4-(trimethyl ammoniummethyl) benzophenone chloride, 2-hydroxy-1-[4-(2-hydroxyethoxy)phenyl-2-methyl-1-propanone), LAP was found to provide the best results probably due to its superior water-solubility and strong absorbance at 365 nm.

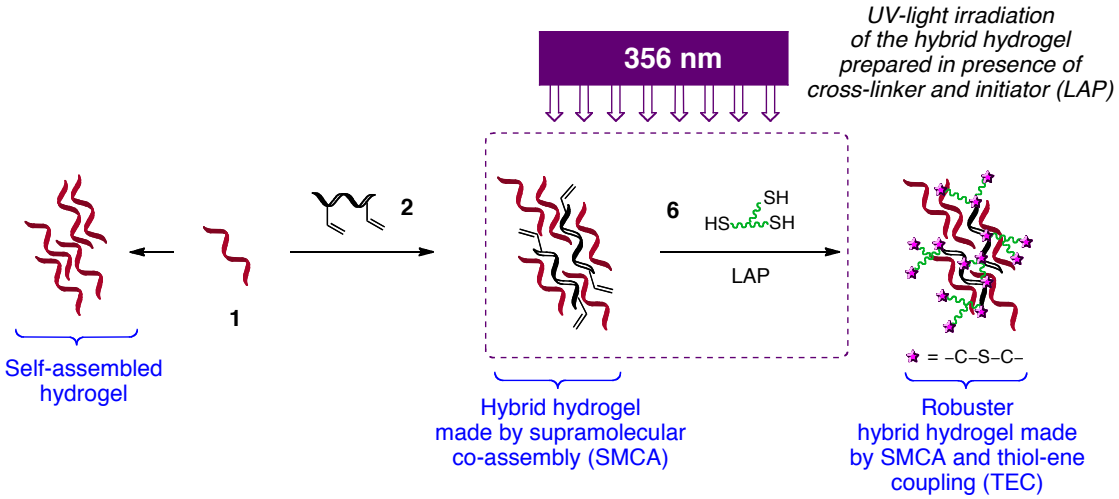

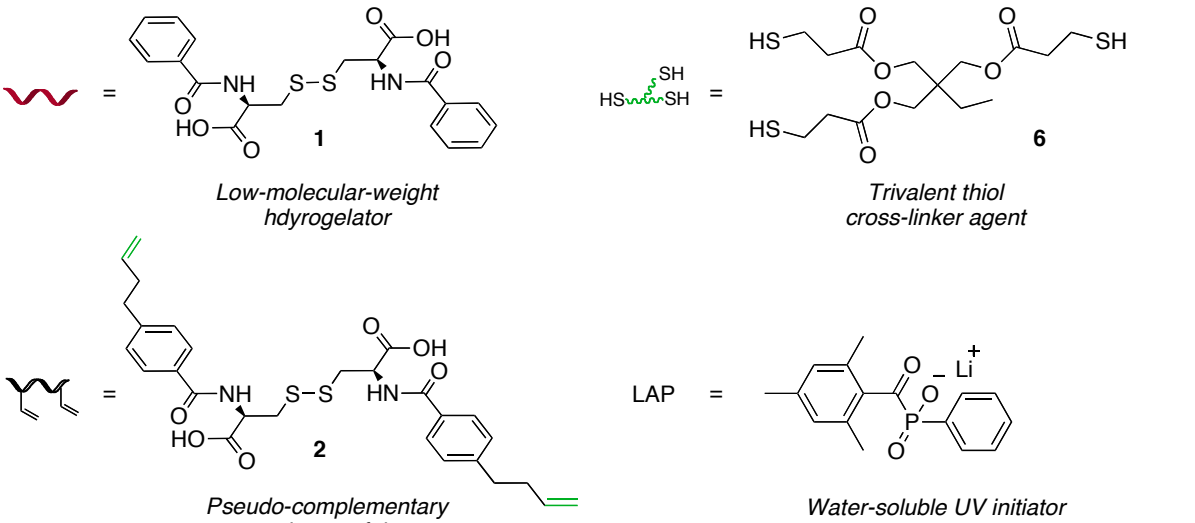

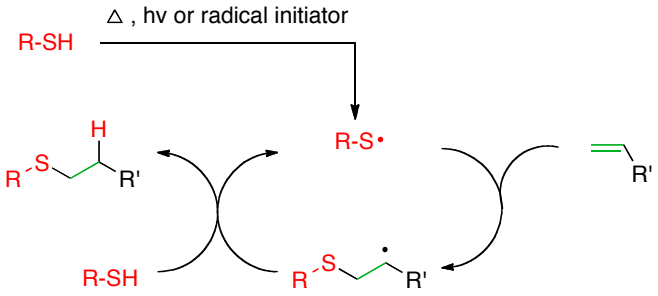

Fig. S2 Illustration of the processes (top) and components (middle) involved in the SMCA-TEC approach. Bottom: Mechanism of the thiol-ene radical reaction.

Among different cross-linkers tested, trivalent thiol **6** was found to be the most effective in terms of thermal and mechanical stabilization followed by PEG-bifunctional thiols (e.g. **5**). Additional thiol-containing cross-linkers were not found to provide any advantage in terms of gel stabilization (Figure S3). Divalent aliphatic thiols (e.g. **9**) where found to be less efficient in the mechanical stabilization of the

hydrogels in comparison with their analogue PEG-containing divalent thiols (e.g. **5**). The use of less flexible divalent aromatic thiols (e.g. **10–11**) resulted in partial crystallization and subsequent destabilization of the gels. Moreover, preliminary experiments showed that both trivalent thiol **12** and isocyanurate trithiol **13** were also effective in the stabilization of the original hydrogel in comparison with trivalent thiol **6** (see main paper), although **6** was finally selected (essentially for availability reasons) as a model compound for the proof of concept. From the results it seems clear that the thiol structure plays a key role in the reaction efficiency and therefore in the stabilization of the nanostructures.

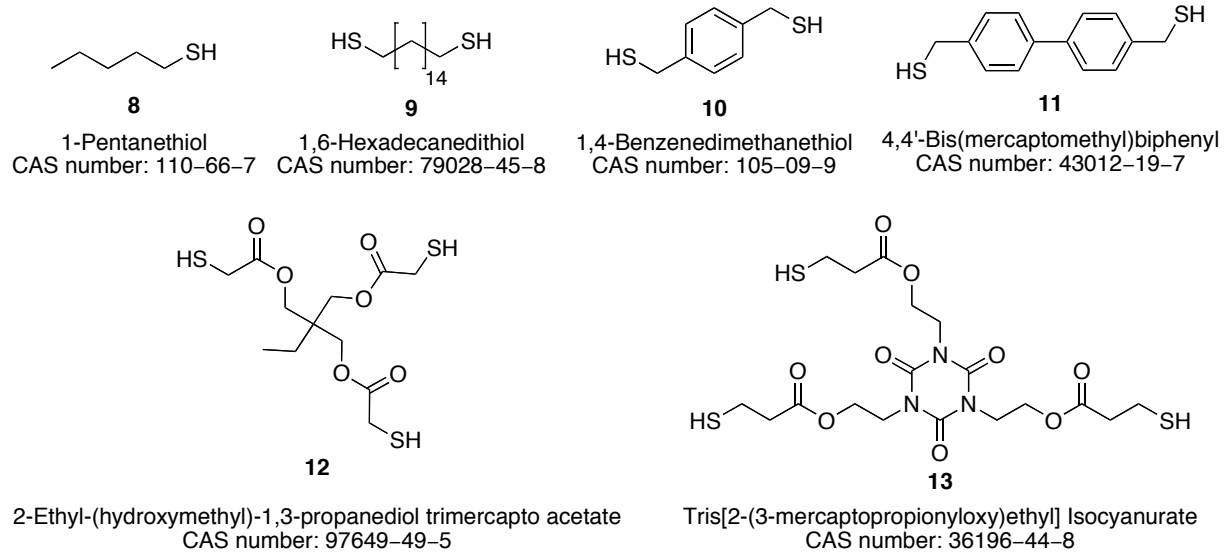

Fig. S3 Additional commercially available thiol-containing cross-linkers evaluated in this work.

In order to calculate the optimum molar ratio between **1** and the corresponding complementary gelator structures, an isotropic solution of the latter was added to an isotropic solution of the former and the system allowed to cool down to promote the formation of the hydrogel. This procedure was repeated at several concentrations of the complementary molecule, maintaining the concentration of **1** constant, until the aggregated material collapsed when the vial was turned upside-down.

- ***Control experiments***

The use of LMWG **1** in the experiments involves important challenges such as maintaining the gelator integrity during the reaction conditions. Being about 40% weaker than C–C and C–H bonds, destabilization of disulfide bonds and deamidation is the main threat for the integrity of both secondary and tertiary structure of the self-assembled hydrogels. In this regard, disulfide linkages in the main chain of poly(amidoamines)s based on *L*-cystine have been shown to be susceptible to both hydrolysis and reductive cleavage, which could represent a valuable alternative to standard degradable systems for triggering the release of encapsulated active substances.[1] The hydrolysis of the activated amidic groups on the above polymers depends mainly on the polymer structure (hindrance next to the amidic group) and pH level. The times for degradation into oligomeric products ranged from 48 h to 2 months. Under an inert atmosphere in a pH 7.4 (TRIS buffer) and 37 ºC, a 10–20% decrease in M_n was observed after 1 day and complete hydrolysis only after 6–7 days. Moreover, in the presence of ca. 5-fold molar excess of 2-mercaptoethanol as reducing agent (model for physiologically reducing environments), a 50% decrease in M_n was observed after 1 day and complete degradation in 2 days.[1] Thiol-disulfide exchange is usually inhibited at low pH where the protonated thiol form is favoured relative to the deprotonated thiolate form. Nevertheless, under the described mild experimental conditions **1** was found to be stable during the duration of the experiments. On the other hand, completion of TEC reaction ensures a thiol-free environment, which contributes to the stability of the modified hydrogels. Disappearance of either the unsaturation signals in the NMR spectrum or standard calorimetric test for free-sulfhydryl (i.e. sodium

nitroprusside) on the crude products was used to confirm full conversion. Unfortunately, the characteristic ν_{SH} band at 2400 cm^{-1} in the IR spectrum was somehow difficult to assign due to the overlap with the broad ν_{OH} band due to the carboxylic groups.

Only those samples submitted to UV light irradiation after SMCA showed a consistent enhancement in their thermomechanical properties. On the other hand, the replacement of the complementary gelator structures (i.e. **2**–**4**) by non-complementary divalent alkenes (i.e. *N*-[Ethyl-2-(5α-cholestan-3β-ylcarbamate)]-3,5-bis(prop-2-ynyloxy)benzamide,[8] *N*-[(1*R*,2*R*)-2-(10-undecynoylamino)cyclohexyl]-10-undecynamide,[9] 1,7-octadiyne) resulted in precipitation rather than gelation upon cooling down the isotropic solution. The use of monofunctional caps such as **8** (Figure S3) instead of cross-linkers did not afford the formation of stable gels.

4. Rheological experiments

Oscillatory rheology experiments were performed with an AR 2000 or Bohlin CVO rheometer to determine the storage modulus (*G′*, elastic component) and loss modulus (*G″*, viscous component) of the samples (Figure S4). The tan δ values (*G″*/*G′*) were reproducible from batch to batch and the materials were considered gels if $G' > G''$. Herein, the kinetics of *in situ* TEC cross-linking and the concentration of the components, as well as the thermodynamics of mixing, control both the gelation and phase separation processes of the SIN-like materials. In general, the material rigidity (*G′*) was found to follow a relative uniform trend with respect to T_{gel} upon TEC. The following experiments were carried out for each sample, using *ca.* 1 mL total gel volume: 1) *Dynamic Strain Sweep (DSS)*: evolution of *G′* and *G″* with strain. The hydrogels were within the linear viscoelastic regime below 1% strain; 2) *Dynamic Frequency Sweep (DFS)*: evolution of *G′* and *G″* with frequency. In general, the hydrogels were viscoelastic for frequencies ranging from 0.1 to 100 rad/sec; 3) *Dynamic Time Sweep (DTS)*: evolution of *G′* and *G″* with time keeping the strain and frequency values constant and within the linear viscoelastic regime (strain = 0.1% strain; frequency = 10 rad/sec, temperature = 20 ºC).

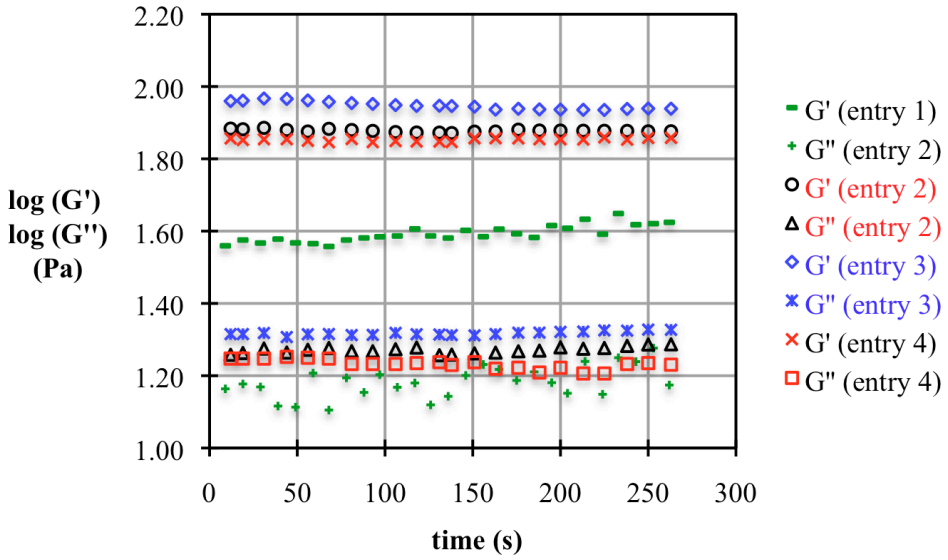

Fig. S4 DTS measurements within the viscoelastic regime of gels outlined in Table 1 of main text.

The storage modulus for the hydrogels made of the mixture **1**+**2**+**5**, **1**+**2**+**6** or **1**+**4**+**6** before UV-irradiation were 58.3, 59.4 and 57.2 Pa respectively, being the tan δ values constant in comparison with the original gel (within the experimental error of these measurements), suggesting that the strength enhancement of the gels takes place upon thiol-ene cross-linking and not only by the simple mixture of the components.

5. Drug encapsulation and release studies.

- ***General remarks***

UV-Vis spectra were recorded with a UV-2101Pc or Varian Cary 50 UV-Vis scanning spectrophotometer. For a specific component, the extinction coefficient (ε, M^{-1} cm^{-1}) was calculated as the average value obtained from three independent measurements at different concentrations (sequential dilution of a stock solution) from which the corresponding linear calibration curve was obtained. UV-active 2-hydroxyquinoline was used as a model drug. The extinction coefficient obtained for 2-hydroxyquinoline at 226 nm in water was 29445.54 M^{-1} cm^{-1}.

- ***Drug release studies***

The designed amount of dried materials and 2-hydroxyquinoline (from a 10^{-6} M stock solution in water) as indicated in the main text were mixed with 1 mL of pure water in a screw-capped glass vial (5 cm length and 1 cm diameter). Hydrogels were reformed by heating until reaching an isotropic solution and further cool down at room temperature and stand for at least 2 h. For any given gel matrix, the concentration values were held constant for each gel system to allow direct comparison between them. For the drug release measurements 1 mL of water as receiving media was carefully placed on top of each hydrogel (non-sink conditions). In order to minimize undesired interactions with the gel network, the above protocol was used to prepare a collection of samples for each hydrogel from which the absorbance of the supernatant solution was recorded at different times. This procedure was found to be more reproducible for the studied materials than taking aliquots from only one sample and resupplying the receiving medium.

The concentration of the 2-hydroxyquinoline, which was released from each hydrogel, was calculated based on the corresponding calibration curves built from the absorbance values at 226 nm. Concentrations of LMWG **1** in supernatants were determined based on its calculated extinction coefficient at 230 nm (19846 M^{-1} cm^{-1}). The percentage release was calculated using the following equation: % release = (Abs of drug molecules released in water/Abs of total molecules encapsulated in gel) × 100. Release of **1** reached a plateau value (ca. 10 molar% respect to the total embedded drug in the gel phase, with a first order constant of 19×10^{-4} s^{-1}) after one day for the unmodified hydrogel (Table 1, entry 1, main paper). Moreover, the release of **1** from modified hydrogels (Table 1, entries 2–4, main paper) was found to be ca. 2-fold slower (before evident degradation of the materials after 14 h), probably due to its stronger retention after TEC cross-linking. Although a systematic study was not performed on the temperature effect, preliminary experiments confirmed the expected increase (ca. 5–10%) of the kinetic release as temperature increase (ca. 10 ºC) below the T_{gel}, and a consistent behaviour of the samples prepared when the drug loading was adjusted below the optimal (1 mM). In addition, the use of slightly different concentrations of gelator **1** (below the crystallization limit) did not affect the release of the drug and the comparative release rates were similar to those reported here. The influence of other receiving medium (different than water) on the drug release rate was not tested in this work.

- ***Diffusion coefficients***

Regardless of the porosity, the Higuchi equations prove that the release rate is directly proportional to the surface area to volume ratios, the total amount of drug incorporated in the matrix (drug loading), the solubility of the drug, and its diffusion coefficient (D) from the gel matrix. In our systems, the diffusion coefficient of the drug in each gel matrix was calculated using the non-steady-state diffusion model equation given below: [25]

$$M_t / M_\infty = 4(D\,t / \pi\,\lambda^2)^{1/2}$$

where M_t is the total amount of drug molecules released during the measurement, M_∞ is the total amount of drug molecules that are kept in the hydrogel matrix, D is the diffusion coefficient of the drug molecule, t is the time of the measurement and λ represents the hydrogel thickness.

6. Electron microscopy

- ***General remarks***

Samples were observed with a Philips CM120 transmission electron microscope operating at an accelerating voltage of 100 kV. Scanning electron micrographs were taken with a Philips XL120 field emission scanning electron microscopes equipped with a digital camera. The accelerating voltage of the scanning electron microscope was 5−20 kV, and the emission current was 10 μA. Copper grids (300 mesh) coated with formvar stabilized with carbon were purchased from Ted Pella, Inc.

- ***Transmission electron microscopy (TEM)***

The specimens were prepared as follow: About 10 μL of the samples were rapidly poured into 100 μL of water. 10 μL of the new suspension was immediately allowed to adsorb for 30 minutes onto copper grids (300 mesh) coated with formvar stabilized with carbon. Excess solvent was removed by touching the edges with a small piece of Whatman paper, and the grids were dried under reduced pressure overnight at room temperature. The relatively large size of the polymer pieces made negative staining unnecessary for visualization (Figure S5).

- ***Scanning electron microscopy (SEM)***

Samples of the xerogels were prepared by the freeze-drying method from their gel phases.[10] A vial (1 mL) containing a piece of the gel was frozen in liquid nitrogen or dry ice/acetone and the sample was immediately evaporated under reduced pressure overnight at room temperature. The resulting fibrous solid was placed on a tin carbon plate and shielded by Pd/Au for 360 s to provide the necessary conductive surface (Figure S5).

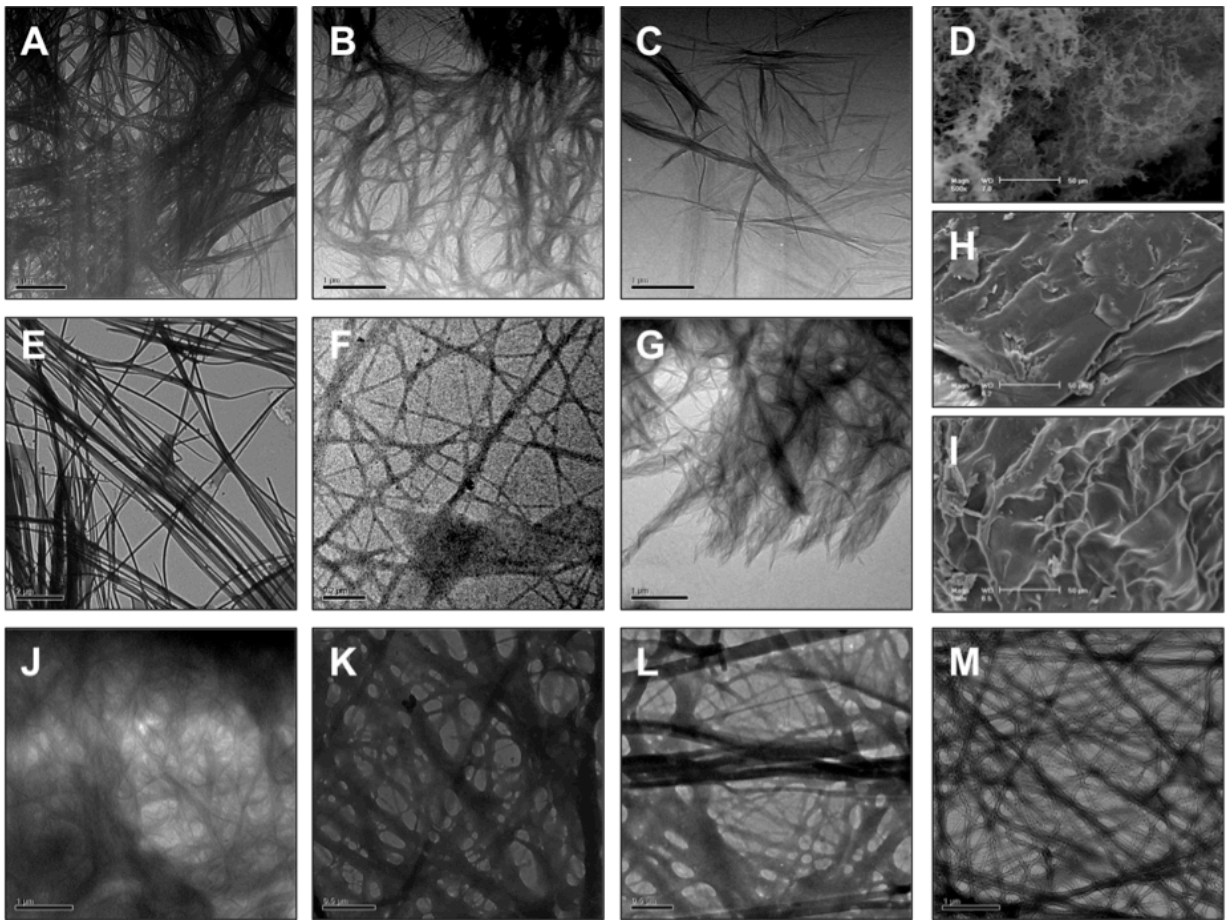

Fig. S5 Additional TEM and SEM images of prepared hydrogels under the conditions described in the main paper: (A, B, C) TEM images at different regions of the gel sample made of **1** (bars: A = B = C = 1 μm). Approximate fiber diameters: 20–120 nm; (D) SEM image of the xerogel from **1**+**2**+**6** (bar = 50 μm) upon irradiation; (E) TEM image of the gel from **1**+**4**+**6** (bar = 2 μm) upon irradiation; (F) TEM image of the gel from SMCA of **1**+**4** (bar = 0.2 μm); (G) TEM image of the gel from **1**+**2**+**3** (bar = 1 μm) upon irradiation; (H, I) SEM images of the xerogel from **1**+**2**+**5** (bars: H = I = 50 μm) upon irradiation; (J) TEM image of the gel from **1**+**2**+**6** (bar = 1 μm) upon irradiation; (K, L, M) TEM image of the gel in (J) but using 2-fold higher concentration of **1** (bars: K = L = 0.5 μm, M = 1 μm) upon irradiation. In general, the presence of overlapped fibers may promote the formation of microdomains and account for the opacity of the gels. On other hand, compacted fibrous character of the sheets in some cross-linked gels could indicate some confined crystallinity.

7. References

1 E. Emilitri, E. Ranucci and P. Ferruti, *J. Polym. Sci., Part A Polym. Chem.,* 2005, **43**, 1404–1416.
2 See reference 16 in the main text.
3 T. Nagasawa, I. Kiyosawa, K. Kawase, T. Suzuki and A. Kawashiri, *Jpn. Kolai Tokkyo Koho*, 1974, JP 49093521.
4 See reference 15 in the main text.
5 See reference 22 in the main text.
6 Benjamin D. Fairbanks, Michael P. Schwartz, Christopher N. Bowman, Kristi S. Anseth, *Biomaterials* 2009, **30**, 6702–6707.
7 J. Samuelsson, M. Jonsson, T. Brinck and M. Johansson, *J. Polym. Sci., Part A Polym. Chem.,* 2004, **42**, 6346–6352, and references therein.
8 D. D. Díaz, J. J. Cid, P. Vázquez and Tomás Torres, *Chem. Eur. J.* 2008, **14**, 9261–9273.
9 See reference 17 in the main text.
10 S. W. Jeong and S. Shinkai, *Nanotechnology*, 1997, **8**, 179–185.